The effects of dye dopants on the conductivity and optical absorption properties of polypyrrole

Eva Håkansson [a], Tong Lin [a], Hongxia Wang [a] and Akif Kaynak [b,]*

a Center for Materials and Fibre Innovation, Faculty of Science and Technology, Deakin University, Geelong, VIC 3217, Australia

b School of Engineering and Information Technology, Faculty of Science and Technology, Deakin University, Geelong, VIC 3217, Australia

Abstract

Ten anionic compounds, including four acidic dyes, were used to dope polypyrrole powder. The effects of the dopants on density, optical absorption and conductivity of the polypyrroles were studied. The presence of the dopant in the conducting polymer matrix was verified by ATR-FTIR spectroscopy. Density function theory (DFT) simulation was used to understand the effect of the dopants on the solid structure, optical absorption and energy band structures. Anthraquinone-2-sulfonic acid doped polypyrrole yielded the highest conductivity. The dye doped polypyrrole showed an enhancement in its UV—VIS optical absorption.

Keywords: polypyrroles; dyes/pigments; UV-vis spectroscopy; molecular modelling; infrared spectroscopy

---

* Corresponding Author. Tel.: +61-3-5227-2909; fax: +61-3-5227-2539.

E-mail address: akaynak@deakin.edu.au (A. Kaynak).

1. Introduction

As a common feature, conducting polymers are semiconductors of wide bandgap or electrical insulators in their native state. The improvement of the electrical conductivity is typically based on incorporation with an anionic compound, normally called “dopant”, into the polymer matrix. The mechanism of improvement in the electrical conduction in polypyrrole (PPY) has been attributed to a redox interaction between the conducting polymer and the dopant [1-3]. Such an ionic interaction also results in other changes such as electrical and optical properties.

Conducting polypyrrole has potential applications in EMI shielding [4-7], super-capacitors[8, 9], chemical sensors [10, 11] heat generation [12, 13], actuators [14, 15] and electrical display devices [16]. Polypyrrole can be doped by anions such as halogen or sulfonate anion, and the doped PPY shows conductivity in the range of 10^{-5} ~ 100 S/cm, depending on the dopant structure and doping method.

Dyes have been traditionally used as colorants. However, due to their unique optical absorption and semi-conductor characteristics [17-20], some dyes have been used as functional materials in optoelectronic devices [21-24] or as optical storage media [25, 26] in CD-ROM or DVD-ROM photo disks. Due to strong π- π interaction and planar structure many dyes have poor solubility. The introduction of solubility-enhancing groups such as sulfonate has been a major strategy to improve the solubility in water, and the sulfonate-containing dyes, often classified as acidic dyes, have broad applications in wool and nylon dyeing. Because of the sulfonate groups, the acidic dyes can be used as dopants in conducting polymers. The large conjugated system of dyes could exert electronic interaction with the π–system of the polypyrrole, which

could lead to a series of changes in the electronic properties of polypyrrole. However, a detailed investigation of incorporation of acidic dye-based dopants into polypyrrole has not been reported.

Molecular simulation has become a powerful tool to aid the experimental scientist in understanding the structure-property relationship of existing materials and predicting the properties of new materials. Work on simulating the solid structure and energy properties of polypyrrole has been reported [1, 2, 27, 28], and has shown comparable results to experimental observations. However, the effect of the structure of dopant on the energy band and electrical properties has not been adequately reported.

In this work, four different acidic dyes and six other anionic dopants were used separately to dope polypyrrole. The doped polypyrroles have been characterized regarding conductivity, density, optical absorption and FTIR spectra. The effect of dye structure on these properties has been studied. Density function theory (DFT) method was used to simulate the dopant-polypyrrole systems for further understanding of the experimental results.

2. Experimental

2.1 Chemicals and methods

Polypyrrole was synthesised using the following dopants: anthraquinone-2-sulfonic acid (AQSA), ferric sulphonate ($Fe_2(SO_4)_3$), para-toluene-2-sulfonic acid (pTSA), dodecylbenzene-2-sulfonic acid (DBSA), ferric bromide ($FeBr_3$), sodium iodide (NaI), Reactive Blue 4 (RB), Nuclear Fast Red (NFR), Naphthol Green B (NG) and

Indigo Carmine (IC). Polypyrrole powders were prepared using an oxidizing system consisting of a ferric salt of dopant anion or a combination of a non-oxidizing dopant anion with ferric chloride. The molar ratio of pyrrole to dopant was fixed at 4:1. Chemical details are listed in Table 1. Dyes were obtained from Aldrich and used as received. Pyrrole (98%, Aldrich) was distilled under vacuum prior to use. All other chemicals were obtained from Aldrich and used as received.

Density measurements were carried out using a helium purged volumetric pycnometer (AccuPyc 1300, Micromeritics), which determines the density and volume of the powder sample by using pressure change of helium in cavity with a calibrated volume. The density was determined to an accuracy of 0.03% of the reading after 10 runs with 90 purges each using a 99.995 % pure Helium gas at a pressure of 22 psig.

ATR- FTIR was carried out using a Fourier Transform Infrared Spectrometer (Bruker Tensor 37). The polypyrrole powders (KBr-pellets) were previously dried under vacuum for more than 7 days. At least three spectra of each polypyrrole powder sample and each reference sample were collected to reduce errors.

Thin discs solely from polypyrrole powder including the different dopants were prepared in a compressor and used for measuring the conductivity. The thickness of the polypyrrole discs was measured using a digital vernier calliper and averaged over 5 or more measurements. Four-probe method was used to determine the conductivity of the discs.

2.2. Synthesis

A temperature controller (DC30 ThermoHaake) and a cooling unit (K20 ThermoHaake) combined with a jacketed water-cooled beaker were used to maintain reaction temperature at 5°C. The pyrrole monomer and ferric-dopant ions were mixed directly in an aqueous solution and stirred at 500 rpm for 6 hours, which gave a black powder suspended in the reaction solution. After filtering and rinsing with deionized water, ethanol and acetone in sequence, the polypyrrole powders were dried in a Binder vacuum oven for 7 days.

2.3. Density Function Theory (DFT) calculation

The solid geometries of polypyrrole were built up with the aid of a computer program, "Amorphous Cell" which is included in the Molecular Studio 2.0 software package. Theory on the construction of an amorphous polymer system used in the Amorphous Cell program has been given in the literature [29-33]. Four repeat units of pyrrole were used in every cell. Ten configurations were considered and the polymer density for the un-doped polypyrrole was set at 1.24 g/cm^3. The density of benzene sulfonate acid (BSA) doped polypyrrole was obtained experimentally. The built solid geometries were subjected to an initial geometric optimization using a Polymer Consistent Force Field (PCFF) method [34-36], that is included in the same program, with a 0.1 Kcal/(mol A) level of convergence. The cell structures were further optimized by using another DFT program (Castep) in the Material Studio 2.0, based on a gradient-corrected (GGA) functional and a revised Perdew-Burke-Ernzerhof functional (RPBE) [37]. The optimized geometries were used to calculate the energy bands, the electronic band structures and the optical absorptions with the same program.

3. Results and discussion

The chemical structures of the dopants are shown in Table 1. The dopants (a-d) are small-molecule organic compounds containing one sulfonic anion each in the molecule. Dopants e and f contain inorganic bromide and iodide anions, respectively, while (g-j) are acidic dyes, which have large bulky molecular structures.

3.1. Polymer densities

The net density measurements are very sensitive to moisture and to the leakage of vacuum chamber; hence the measurements had to be repeated until a satisfactory accuracy was obtained. The density measurements on polypyrrole powders had a small standard deviation (less than 0.5 %), except for the ferric bromide doped polypyrrole powder, of which the standard deviation was around 3% because of a relatively small volume used in the test.

As listed in Table 1, the density of the polypyrrole powders show slight differences depending on the structure and molecular weight of the dopant employed. The polypyrrole powders doped by sulfonic acid, anthraquinone-2-sulfonic and dodecylbenzene sulfonate acid show closely spaced density values, ranging from 1.2 to 1.4 g/cm^3. They have the lowest densities among the PPY powders tested. Due the high atomic weight of iodide (126.90447 g/mol) and compact structure, the PPY powder doped with the iodide ion has the largest density value, exceeding 1.6 g/cm^3. The bromide doped PPY would have a similar matrix structure to the iodide doped PPY, with the former having a slightly lower density value (1.469 g/cm^3) than the

latter, due to the effect of atomic weight on the density. There is not much variation in the density among the PPY powders doped by the four different acidic dyes. The standard deviations are all less than 0.11%, indicating that the measurements have good accuracy.

3.2. FTIR Spectra

To confirm the existence of the dopant molecules in the polypyrrole powders, FTIR spectra of the dopant and the doped polypyrrole powders were compared. Due to the strong and broad vibration bands of polypyrroles, only small differences can be observed between the spectra with and without the dopant molecule. Figure 1 shows spectra of the fingerprint region for the polypyrrole made by using only the oxidant, ferric chloride and is in good agreement with earlier investigations of the same product [38-42].

Assignments for polypyrrole and corresponding vibration modes are shown in Figure 1 [43]. The broad C=C stretching band at around 1550 cm^{-1} were observed to change as the polypyrrole was doped with different anions (Figure 2). The addition of a quinone structure, e.g. AQSA, shifts the absorption towards lower wave numbers (1538 cm^{-1}), whilst the anionic dye (Naphthol Green B, NG) and the small ferric bromide dopant shifts the absorption towards higher wave numbers (1563 and 1558 cm^{-1} respectively). These results are in accordance with data reported in literature [44].

Figure 3 displays a few differences between systems a-d, all of which contain a sulfonic group. Solid arrows indicate significant changes compared to ferric chloride (bottom spectra) and dashed arrows indicate locations where dopant-related peaks are obscured by the polypyrrole spectra itself.

In the PPY-AQSA powder, absorption around 750, 1250 and 1690 cm^{-1} can be detected and related to the incorporation of AQSA. An expected AQSA-related peak at 1710 cm^{-1} is obscured. The PPY-DBSA shows broadening of the band at 670 cm^{-1} and a small overlapping peak at around 1010 cm^{-1}. Expected strong DBSA absorptions at 1200 cm^{-1} and 1470 cm^{-1} are obscured. Broader absorption bands at 900 and 1230 cm^{-1} for PPY-$Fe_2(SO_4)_3$ as well as slight increase of absorption at 690 and 830 cm^{-1} for PPY-pTSA is attributed to the respective dopants. Strong absorption from sulphur-oxygen stretching for pTSA at around 1150cm^{-1} is obscured by the PPY [40].

The addition of sodium iodide and ferric bromide (systems e and f) as oxidants/dopants does not produce any identifiable peaks for the dopants in the FTIR spectra since they are non-polar in nature. The bulky dye-structures used as dopants in systems g-j are still masked by PPY absorptions, hence it is difficult to isolate absorption bands exclusive to the dyes. However, small differences between the spectra indicate existence of dye-dopant in the polypyrrole powders, as can be seen in Figure 4.

PPY-RB shows a few absorption bands in the region 600-870 cm^{-1} and a slightly obscured peak at 1030 cm^{-1}, which originates in the RB dopant. Expected RB absorptions at 1238, 1295 (1,4-disubstituted aromatics) and 1550 – 1620 cm^{-1} are obscured. PPY-NFR indicates the existence of the dopant in PPY by overlapping peaks at 1340 and 1452 cm^{-1}. PPY-NG system shows absorptions at 674, 1040 and 1210 cm^{-1}, which originate in the pure NG. Peaks at 1032 cm^{-1}, 1600-1660 cm^{-1} and an increase in the 1100 cm^{-1} originate in the pure IC in the PPY-IC system.

3.3. Optical absorption

The UV-VIS absorption for all four dye doped polypyrrole powders shows an increase in the absorption intensity in the whole visible wavelength range as can be seen in Figure 5. In this figure the dashed lines show the signal for the pure dye solution and the solid lines show the response for the dye doped PPY powders. Irrespective of dye incorporated, an absorption peak at 580 nm was observed for all doped PPYs, and broad absorption throughout the rest of the visible range, which is an attribute of the dark color of the oxidized PPYs. The UV-VIS signal for all PPY powders look similar irrespective of dye incorporated. However, the absorption peaks of the dyes can still be observed for some of the tested PPY powders, which further confirm the existence of the dyes in the polymer matrix.

3.4. Conductivity

Table 1 gives the conductivities of polypyrrole powders made with different dopants. As expected, the highest conductivity was obtained in the PPY-AQSA system [45], which may be attributed to the planar structure of the AQSA molecule. This was closely followed by the other systems incorporating a sulfonic anion, experimental result of which is in accordance with the smaller bandgap modelled for the benzene sulfonate anion. This is discussed further in the next section. The ferric salt $Fe_2(SO_4)_3$ has the second highest conductivity, indicating that the simultaneous oxidation and dopant function is successful.

All the PPY samples containing acidic dyes show significant conductivity, which is encouraging for the future exploration of the acidic dyes as dopants. However, the conductivity is generally lower for dye-doped PPY than PPY doped by sulfonic anions. The lower conductivity for the other dye-based dopants is attributed to the

more bulky structure of the dye dopants. The lowest conductivity was exhibited by the PPY powder doped with Naphthol Green B, which is also the largest dye-dopant molecule. The second lowest conductivity was displayed by PPY doped with Indigo Carmine that contains double sulfonic acid groups, which perturbs the arrangement of polypyrrole chains. The change in the molecular arrangement within PPY matrix leads to decrease in the intermolecular interaction that resulted in lower conductivity. On the other hand, the smaller dye molecules, Reactive Blue 4 and Nuclear Fast Red have resulted in higher PPY conductivities. These observations suggest a size dependence of the dopant on the final properties of the PPY. However, it is also important to remember that the dyes contain a certain degree of impurities, which may influence conductivity. The small inorganic anions of ferric bromide and sodium iodide result in PPY conductivities, which are located between the sulfonic and acidic dye doped PPY systems.

The optimized cell geometries for different dopants (Table 2) indicate an increase in cell volume with the addition of dopants. Larger dopants result in larger unit cell volumes. However, the introduction of dopant enhances the intermolecular interaction among the PPY molecules. The doped PPY has much higher conductivity than that without any dopant, but when very large dye-molecules are added as dopants the intra-chain transport of charge carriers may be restrained due to increase in the intermolecular distance, causing a reduction in conductivity. It is suggested that small dopants such as chloride ions or benzene sulfonic acid have little effect on the molecular matrix.

3.5. Density Function Theory Simulations

The "Amorphous Cell" program yields the most probable structure of the modelled material occurring in the solid state. In this study, the lattice parameters were optimized in the amorphous cell calculation. Further DFT optimization only adjusted the molecular structure and relative positions, without changing the lattice parameters. Due to extensive computer time involved in these large calculations, the simulation work was limited to include three typical structures, which are undoped PPY (PPY), Cl-ion doped PPY (PPY-Cl) and benzenesulfonate doped PPY (PPY-BSA) respectively. The optimized geometries of the three polypyrroles and their lattice parameters are listed in Table 2.

The distance between the dopant molecule and the polypyrrole macromolecule are different for each dopant, as indicated in Scheme 1, where the distances between the counterion and the nearest pyrrole ring are indicated. The Cl-anion is located almost along the direction of the N-H bond in the nearest pyrrole ring and the distance of H-Cl and N-Cl are 2.570Å and 3.57Å, respectively. The N-H-Cl angle is 167.056°. However, for the benzene sulfonate anion two oxygen atoms of the sulfonate group approach two different N-atoms of adjacent pyrrole rings. The O-N distances are 3.58Å and 3.05Å, which are comparable to the N-Cl distance. In addition, the O-C1 distances were shorter than Cl-C1. This result suggests that the sulfonate anion could have a larger interaction with polypyrrole linkage than the chloride anion. With the incorporation of BSA into the polypyrrole matrix, the cell value increased considerably due to a larger number of atoms included in the cell unit. For PPY-BSA, two oxygen atoms of the sulfonate group approach two different N-atoms of adjacent pyrrole rings. The O-N distances are 3.58Å and 3.05Å.

The band structure of PPY is shown in Figure 6. Clearly, an energy gap appears between the conduction and the valence bands. The smallest gap value is about 2.092 eV. This result indicates that the un-doped polypyrrole is a semi-conducting material in nature. When the polypyrrole was doped, both the band structure and density of states (DOS) altered. The influence of the dopant on the band structure can be attributed to the redox interaction between the dopant and polypyrrole. The band gap, which is the energy gap between the conduction and the valence bands, is affected by the incorporation of the dopants into PPY.

If the probability (p) that an electron reaches the conduction band is less than 10^{-24}, no single electron can be found in the conduction band in 1 cm^3 solid, and the material tends to be an insulator. The minimal band gap based on this probability value at 25^{o}C (2kT =0.05 eV) is 2.8 eV. The material with band gap between 2.8 eV and zero is a semiconductor. The band gap values for the undoped PPY, PPY-Cl and PPY-BSA were calculated as 2.002 eV, 2.540 eV and 1.941 eV respectively. Therefore, based on their band gap, the semi-conducting nature of all investigated polypyrroles was concluded from this calculation in accordance with the experimental observation. However, it is important to keep in mind that this energy value might be slightly over-estimated as a result of the DFT method of calculation.

More electrons jump to the conduction band due to the existence of dopant, leading to increase in conductivity. The polypyrrole doped by sulfonate anion shows a narrower bandgap than that doped by chloride anion, which is the reason for the relatively higher conductivity of BSA-doped PPY than those doped by other dopants.

The solid optical absorption spectra for the PPY, PPY-Cl and PPY-BSA systems are shown in Figure 7. The undoped polypyrrole shows optical absorptions with peaks at 150 nm, 207 nm and 480 nm. The addition of dopants resulted in red-shift for the first two peaks and blue-shift for the third absorption peak. It is reasonable to expect that dopants with larger aromatic molecules, such as dyes, have larger influence on the optical absorption, which will be confirmed in the future work.

4. Conclusion

In this work, sulfonic acid based dopants, inorganic dopants and acidic dyes were used to dope polypyrrole. Anthraquinone-2-sulfonic acid doped PPY possessed the highest conductivity. The increase in conductivity with the addition of dyes confirmed the doping function of the dyes on polypyrrole. The bulkiest dye-molecule, Naphthol Green B, resulted in the lowest conductivity value indicating possible geometry effects of dopant on the final product. Existence of the dopants in the PPY powders, including dye molecules, was confirmed by ATR-FTIR spectroscopy and UV-VIS absorption. Dye specific peaks were detected by UV-VIS absorption in all dye-doped PPY powders. Further work will focus on studying the optical response of conductivity change upon the dye doped polypyrrole, and effect of other dye-based dopants on properties of conducting polymers.

References

[1] K. Veluri, J. Corish, D.A. Morton-Blake, F. Beniere. Theochem 365 (1996) 13.

[2] K. Veluri, J. Corish, D.A. Morton-Blake, F. Beniere. Theochem 334 (1995) 109.

[3] J. Corish, D.A. Morton-Blake, K. Veluri, F. Beniere. Theochem 102 (1993) 121.

[4] E. Ruckenstein and J.S. Park. Polym. Comp. 12 (1991) 289.

[5] J. Joo and A.J. Epstein. Appl. Phys. Lett. 65 (1994) 2278.

[6] K. Naishadam. IEEE T Elegtromagn. Comp. 34 (1992) 47.

[7] S.H. Kim, S.H. Jang, S.W. Byun, J.Y. Lee, J.S. Joo, S.H. Jeong, J.S. Park. J Appl Pol Sci 87(2003) 1969.

[8] Y. Kudoh, S. Tsuchiya, T. Kojima, M. Fukuyama, S. Yoshimura. Synth. Met. 41 (1991) 1133.

[9] S. Ghosh, O. Inganas. Adv. Mater. 11(1999) 1214.

[10] S. Dong, Z. Sun, Z. Lu. J. Chem. Soc., Chem. Commun. (1988) 993.

[11] F. Selampinar, U. Akbulut, M.Y. Ozden, L. Toppare. Biomaterials 18 (1997) 1163.

[12] E. Hakansson, A. Kaynak, T. Lin, S. Nahavandi, T. Jones, E. Hu. Synth. Met. 144(2004) 21.

[13] K. Kukkonen, T. Vuorela, J. Rantanen, O. Ryynanen, A. Siili, J. Vanhala. "The design and implementation of electrically heated clothing" Proc. Fifth international symposium on wearable computers (2001) 180.

[14] M.R. Gandhi, P. Murray, G.M. Spinks, G.G. Wallace. Synth. Met. 73(1995) 247.

[15] A. Hutchinson, T. Lewis, S. Moulton, G. Spinks, G.G. Wallace. Synth. Met. 113 (2000) 121.

[16] M. Granstrom, K. Petrisch, A.C. Arias, A. Lux, M.R. Andersson, R.H. Friend. Nature 395(1998) 257.

[17] V. Vasey, M.I. Stephenson. J. Phys. D: Appl. Phys. 26(1993) 89.

[18] N.A. Davidenko, N.A. Derevyanko, A.A. Ishchenko, N.P. Vasilenko, P.S. Smertenko, L.I. Fenenko. Theor. Exp. Chem. 37(2001) 338.

[19] S. Bhattacharyya, E. Kymakis, G.A.J. Amaratunga. Chem. Mater. 16 (2004) 4819.

[20] H.-B. Sun, T. Tanaka, K. Takada, S. Kawata. Appl. Phys. Lett. 79 (2001) 1411.

[21] N.A. Davidenko, V.A. Pavlov, N.G. Chuprina, N.A. Derevyanko, A.A. Ishchenko, A.D. Al-Kadimi, V.A. Pivtorak. J Appl. Spectro. 69 (2002) 103.

[22] F.-Y. Li, C.-H. Huang, L.-P. Jin, D.-G. Wu, X.-S. Zhao. J. Mater. Chem. 11 (2001) 3002.

[23] N. Zheng, X. Bu, P. Feng. J. Am. Chem. Soc. 124 (2002) 9688.

[24] A. Niko, S. Tasch, F. Meghdadi, C. Brandstatter, G. Leising. J. Appl. Phys. 82 (1997) 4177.

[25] M. Ushamani, K. Sreekumar, C.S. Kartha, R. Joseph. J. Mod. Opt.51 (2004) 743.

[26] K.E.E. A. N. Burgess, M. Mackay, S. J. Abbott. J. Appl. Phys. 61 (1987) 74.

[27] G. Paasch, D. Schmeisser, A. Bartl, H. Naarmann, L. Dunsch, W. Goepel. Synth. Met. 66 (1994) 135.

[28] M. Breza, V. Laurinc. Macromol. Theor. Simul. 5 (1996) 107.

[29] H.J. Meirovitch. Macromolecules 18 (1985) 569.

[30] M.N. Rosenbluth, A.W. Rosenbluth. J. Chem. Phys. 23 (1955) 356.

[31] D.N. Theodorou, U.W. Suter. Macromolecules 18 (1985) 1467.

[32] R.H. Boyd. Macromolecules 22 (1989) 2477.

[33] D. Rigby, R.J. Roe. J. Chem. Phys. 87 (1987) 7285.

[34] H. Sun, S.J. Mumby, J.R. Maple, A.T. Hagler. J. Amer. Chem. Soc. 116 (1994) 2978.

[35] H.J. Sun. Comp. Chem. 15 (1994) 752.

[36] H. Sun. Macromolecules 28 (1995) 701.

[37] B. Hammer, L.B. Hansen, J.K. Norskov. Phys. Rev. B59 (1999) 7413.

[38] A. Mohammadi, M.-A. Hasan, B. Liedberg, I. Lundstrom, W.R. Salaneck. Synth. Met. 14 (1986) 189.

[39] A. Kaynak, L. Rintoul, G.A. George. Mat. Res. Bull. 35 (2000) 813.

[40] J. Wang, K.G. Neoh, E.T. Kang. Thin Solid Films 446 (2004) 205.

[41] L. Dall'Acqua, C. Tonin, R. Peila, F. Ferrero, M. Catellani. Synth. Met. 146 (2004) 213.

[42] M. Omastova, M. Trchova, J. Kovarova, J. Stejskal. Synth. Met. 138 (2003) 447.

[43] J.M. Davey, S.F. Ralph, C.O. Too, G.G. Wallace. Synth. Met. 99 (1999) 191.

[44] H.H. Kuhn, A.D. Child, W.C. Kimbrell Synth. Met. 71 (1995) 2139.

Captions to Figures/Scheme/Tables

Table 1. Dopants, reactant concentrations, net densities and conductivity of doped polypyrroles.

Table 2. The cell parameters of optimized geometries for solid polymer structure.

Fig. 1. FTIR-ATR spectra of polypyrrole made by solution polymerization with ferric chloride (C_{FeCl_3} = 0.036 mol/l) used as the oxidant.

Fig. 2. FTIR-ATR for polypyrrole powders made from four dopant systems; anthraquinone-2-sulfonic acid, ferric bromide, Naphthol Green B and the reference ferric chloride.

Fig. 3. FTIR-ATR absorption spectra for polypyrrole powders made from systems a-d. AQSA = anthraquinone-2-sulfonic acid, DBSA = Dodecylbenzene sulfonic Acid, ferric Sulphonate, pTSA = para-Toluene-2-Sulfonic Acid. $FeCl_3$ = Reference spectra given by PPY oxidized by $FeCl_3$, without incorporating any other dopant.

Fig. 4. FTIR-ATR absorption spectra for polypyrrole powders made from systems g-j. RB= Reactive Blue 4, NFR = Nuclear Fast Red, NG = Naphthol Green B, IC = Indigo Carmine, $FeCl_3$ = Reference spectra given by PPY oxidized by $FeCl_3$, without incorporating any other dopant.

Fig. 5. UV-VIS Spectra for pure dyes (dashed lines) and for PPY powders doped with different dyes (solid lines). Dyes used are Reactive Blue (a), Nuclear Fast Red (b), Naphthol Green B (c) and Indigo Carmine (d).

Fig. 6. Band structure and DOS of PPY, PPY-Cl and PPY-BSA.

Fig. 7. Optical absorption of polypyrrole in the solid state with different dopants.

Scheme 1. The inter-atomic distances in the optimized cell geometries of PPY-Cl and PPY-BSA. All distances in [Å].

Tables

Table 1.

	Dopants	Dopant Structure	Dopant M_W (g/mol)	N_{dopant} (mol)	$N_{Monomer}$ (mol)	$N_{Ferric\ ion}$ (mol)	Density (g/cm^3)	Std Dev density	Conductivity (S/cm)
a	Anthraquinone-2-sulfonic Acid	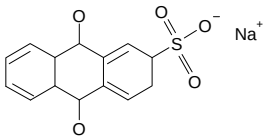	328.28	0.0025	0.01	0.036	1.451	$1.2 \cdot 10^{-3}$	$6.00 \cdot 10^{-3}$
b	Ferric Sulphonate	$Fe_2(SO_4)_3 \cdot xH_2O$	399.88	0.036	0.01	-	1.474	$4.0 \cdot 10^{-3}$	$4.94 \cdot 10^{-3}$
c	para-Toluene-2-Sulfonic Acid	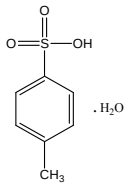	194.18	0.0025	0.01	0.036	1.388	$5.0 \cdot 10^{-3}$	$1.04 \cdot 10^{-3}$
d	Dodecylbenzene-2-Sulfonic Acid	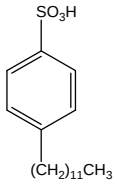	348.48	0.0025	0.01	0.036	1.219	$6.0 \cdot 10^{-4}$	$6.62 \cdot 10^{-4}$

e	Ferric Bromide	$FeBr_3$	295.56	0.0144	0.004	-	1.469	$3.0 \cdot 10^{-2}$	$5.84 \cdot 10^{-4}$
f	Sodium Iodide	NaI	149.89	0.0025	0.01	0.036	1.693	$3.7 \cdot 10^{-3}$	$2.01 \cdot 10^{-4}$
g	Reactive Blue 4	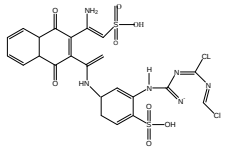	637.44	0.025	0.01	0.036	1.411	$1.1 \cdot 10^{-3}$	$7.27 \cdot 10^{-4}$
h	Nuclear Fast Red	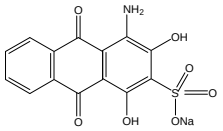	357.27	0.025	0.01	0.036	1.520	$7.0 \cdot 10^{-4}$	$4.70 \cdot 10^{-4}$
i	Naphthol Green B	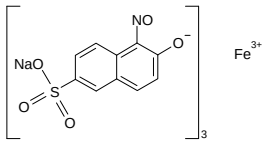	878.47	0.025	0.01	0.036	1.476	$9.0 \cdot 10^{-4}$	$8.73 \cdot 10^{-5}$
j	Indigo Carmine	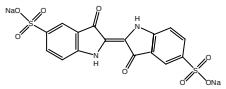	466.35	0.025	0.01	0.036	1.487	$9.4 \cdot 10^{-4}$	$6.02 \cdot 10^{-5}$

Table 2.

Polypyrrole	Lattice Structure	Lattice Parameters						Volume
		A	B	C	α	β	γ	A^3
PPY	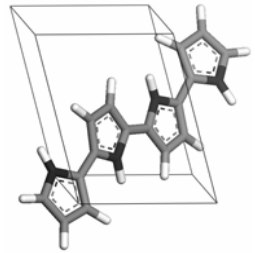	6.036220	7.433580	7.429840	75.444470	102.408350	81.983190	308.473914
PPY-Cl	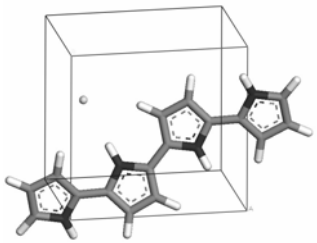	8.628340	7.954570	7.110570	59.037890	116.408800	91.938400	362.536699
PPY-BSA	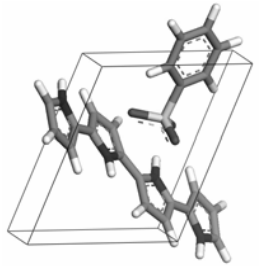	8.327370	8.733310	8.689040	93.816870	106.085120	119.662210	511.670334

Figures

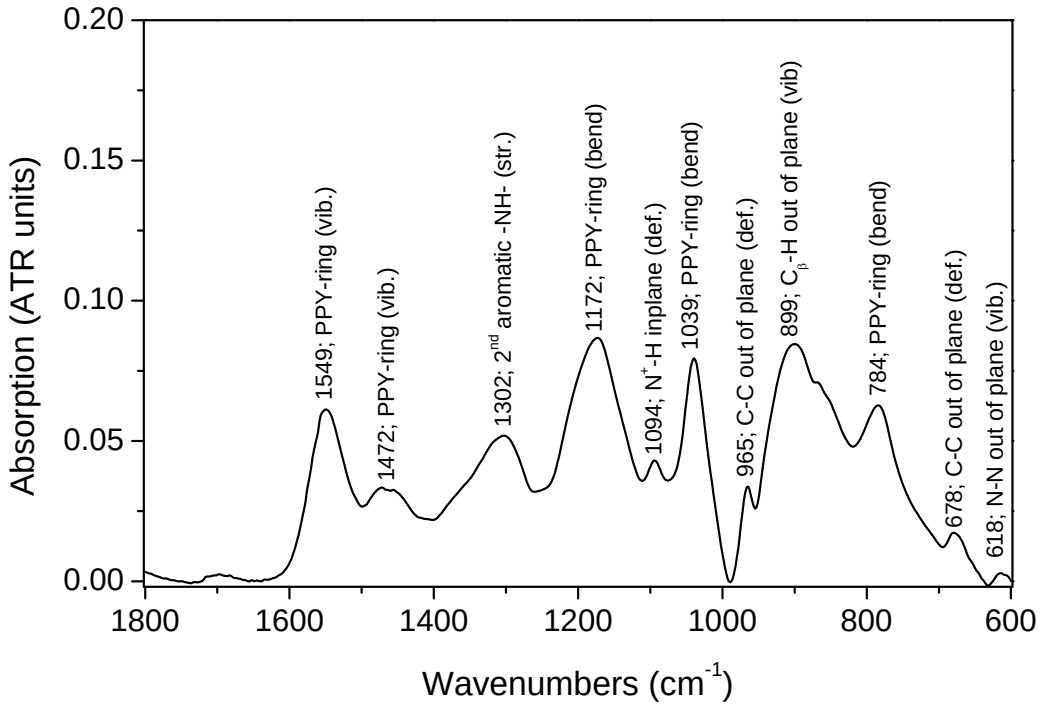

Fig. 1. FTIR-ATR spectra of polypyrrole made by solution polymerization with ferric chloride (C_{FeCl_3} = 0.036 mol/l) used as the oxidant.

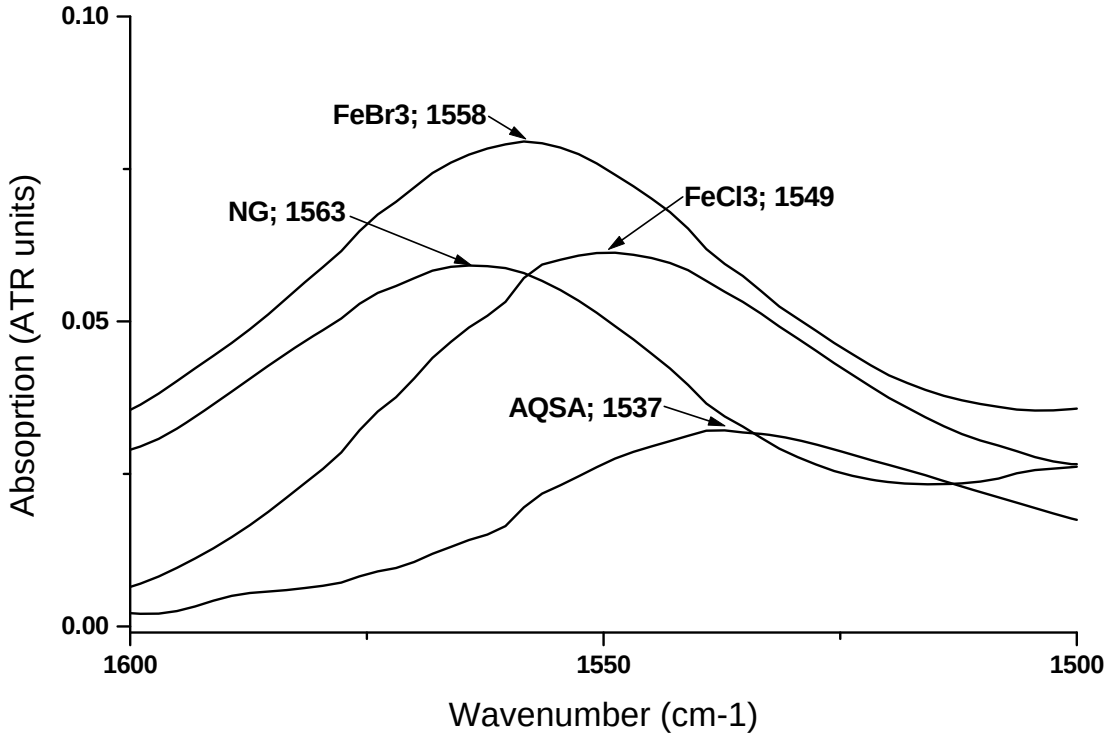

Fig. 2. FTIR-ATR for polypyrrole powders made from four dopant systems; anthraquinone-2-sulfonic acid, ferric bromide, Naphthol Green B and the reference ferric chloride.

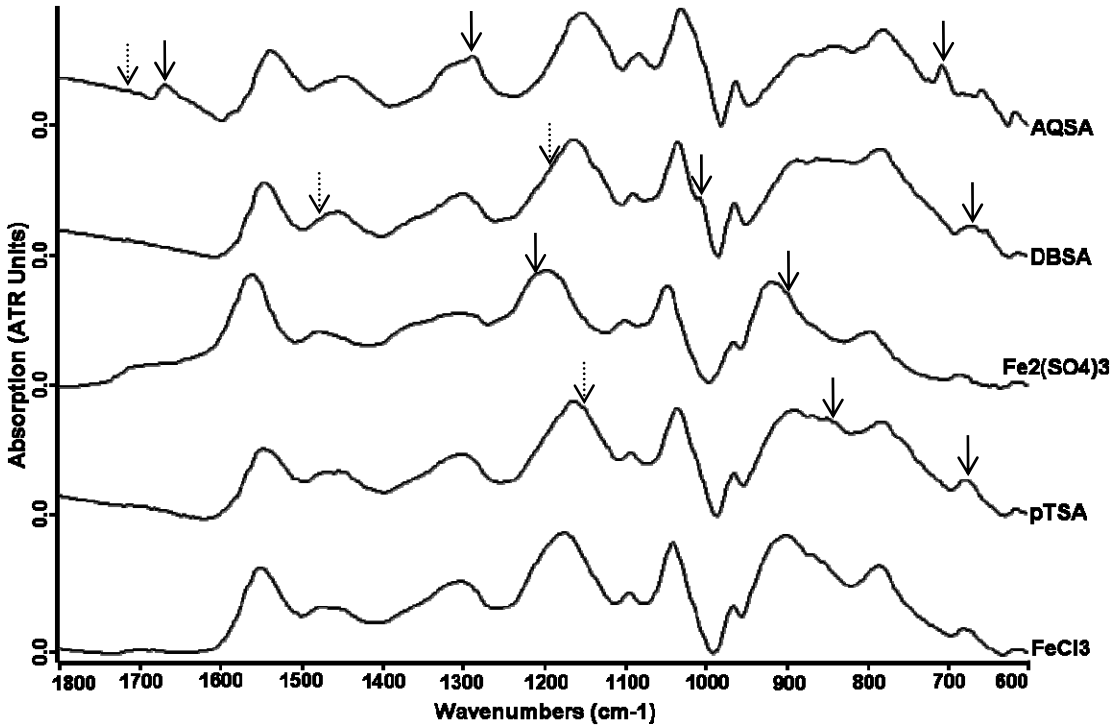

Fig. 3. FTIR-ATR absorption spectra for polypyrrole powders made from systems a-d. AQSA = anthraquinone-2-sulfonic acid, DBSA = Dodecylbenzene sulfonic Acid, ferric Sulphonate, pTSA = para-Toluene-2-Sulfonic Acid. $FeCl_3$ = Reference spectra given by PPY oxidized by $FeCl_3$, without incorporating any other dopant.

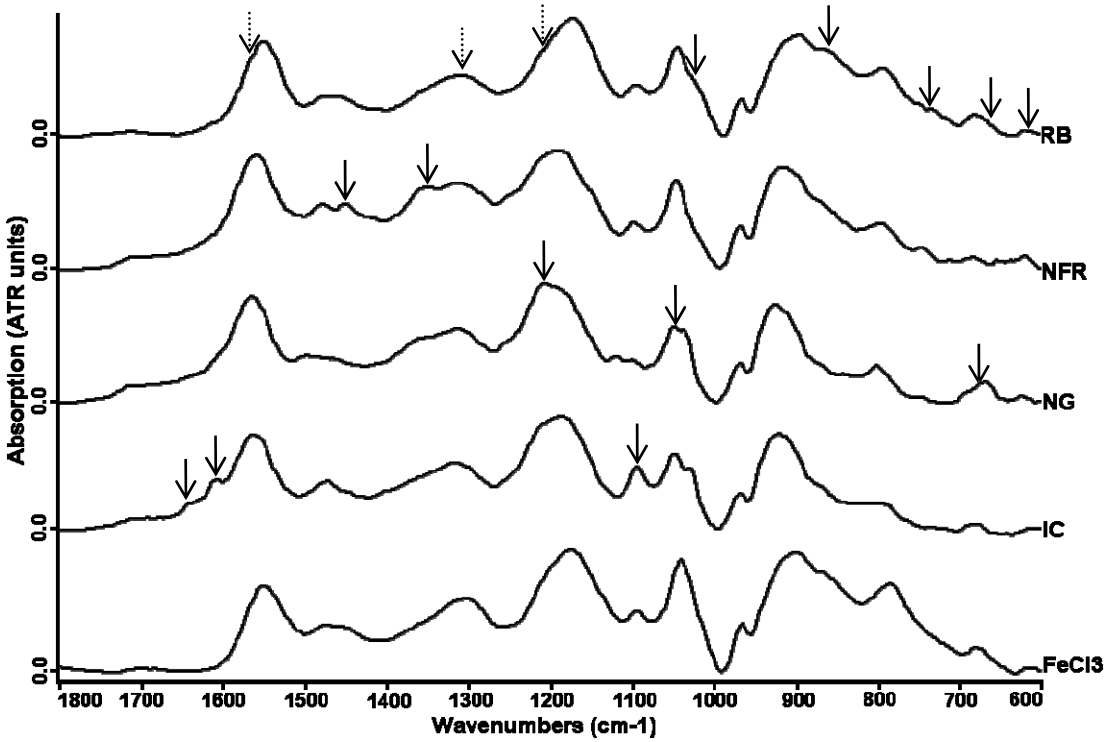

Fig. 4. FTIR-ATR absorption spectra for polypyrrole powders made from systems g-j. RB= Reactive Blue 4, NFR = Nuclear Fast Red, NG = Naphthol Green B, IC = Indigo Carmine, $FeCl_3$ = Reference spectra given by PPY oxidized by $FeCl_3$, without incorporating any other dopant.

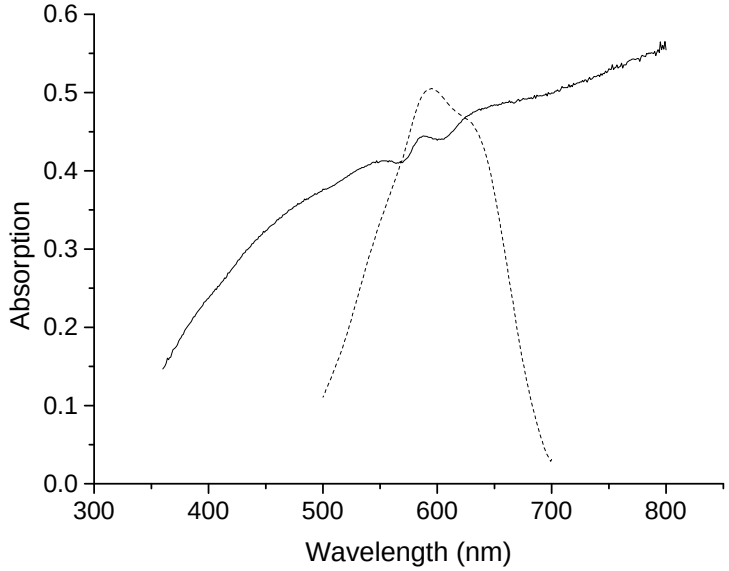

a) Reactive Blue 4

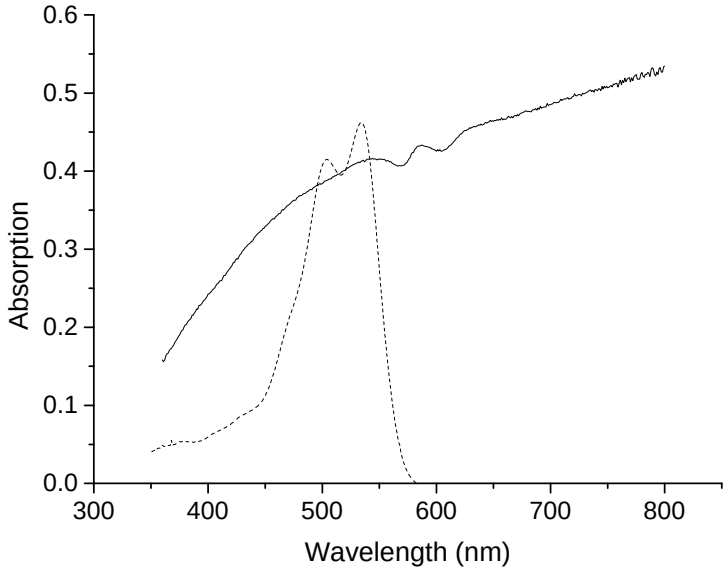

b) Nuclear Fast Red

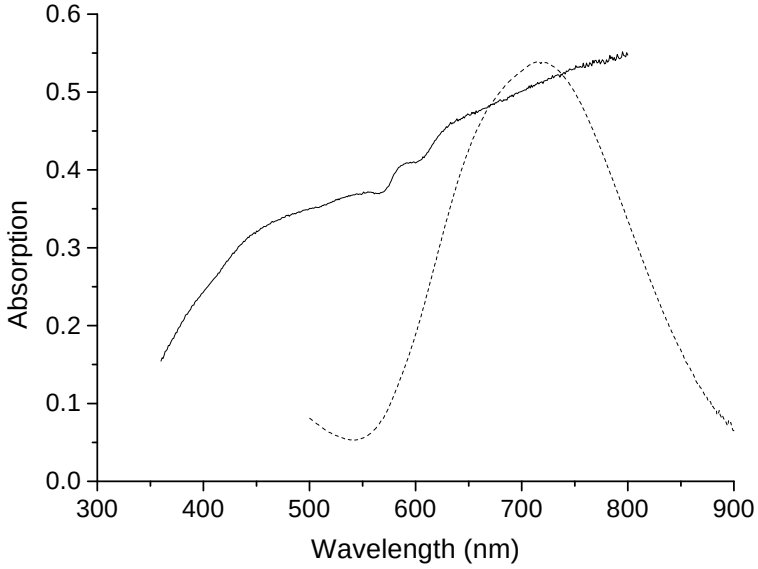

c) Naphthol Green B

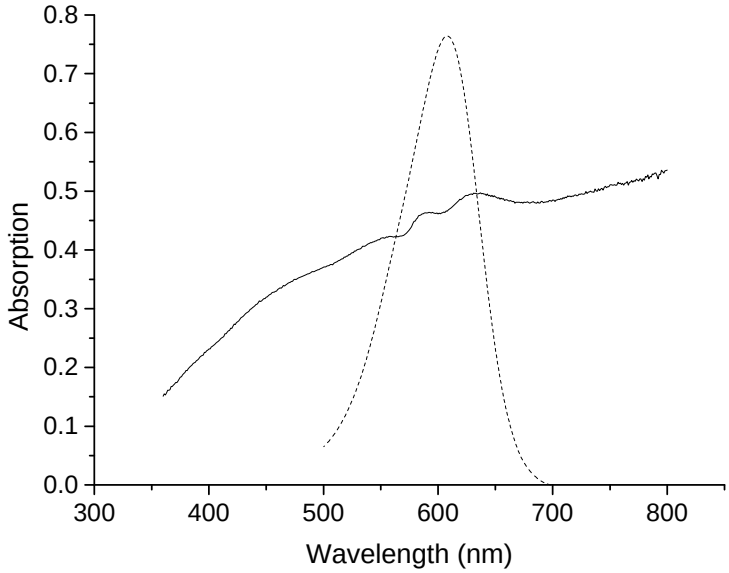

d) Indigo Carmine

Fig. 5. UV-VIS Spectra for pure dyes (dashed lines) and for PPY powders doped with different dyes (solid lines). Dyes used are Reactive Blue (a), Nuclear Fast Red (b), Naphthol Green B (c) and Indigo Carmine (d).

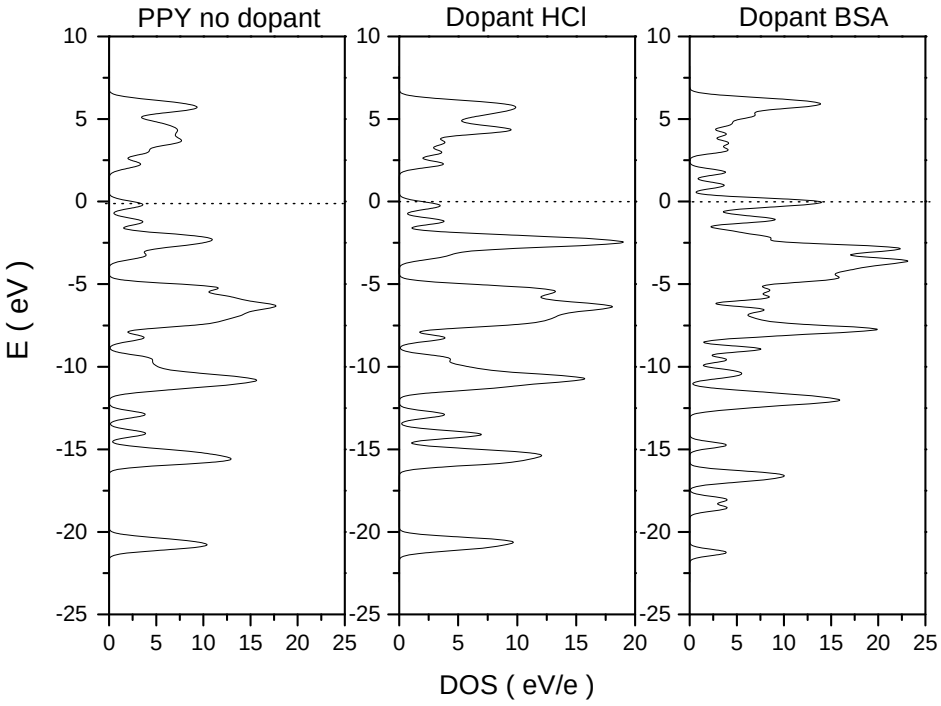

Fig. 6. Band structure and DOS of PPY, PPY-Cl and PPY-BSA.

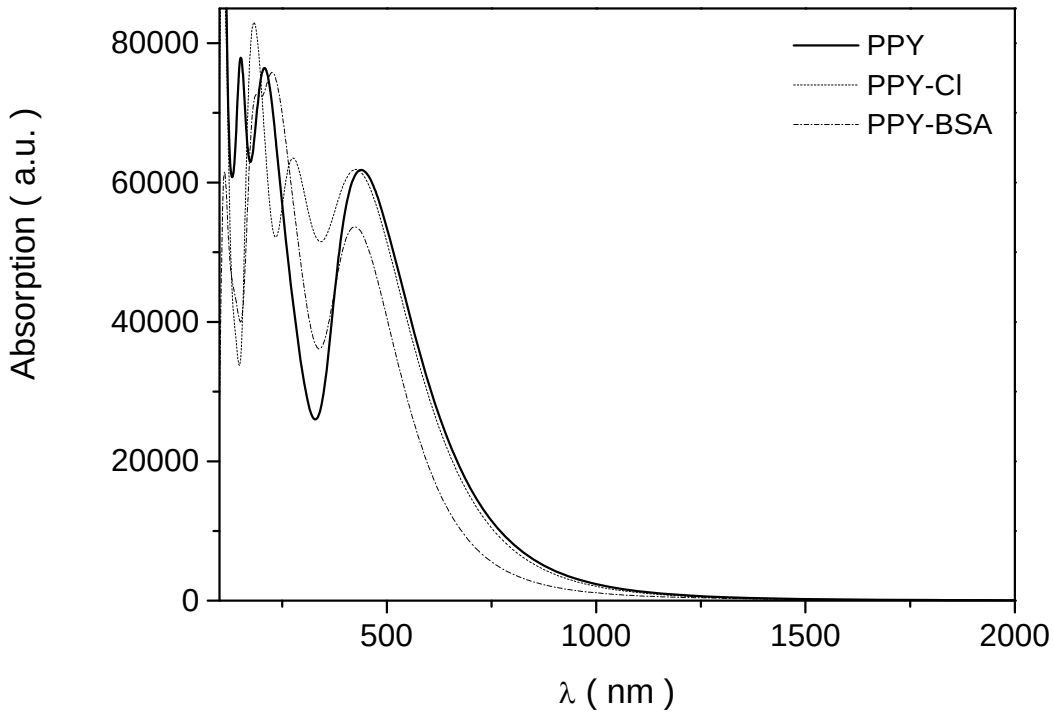
Absorption (a.u.)
80000
60000
40000
20000
0
500
1000
1500
2000
λ (nm)
PPY
PPY-Cl
PPY-BSA

Fig. 7.

Scheme

Scheme 1.

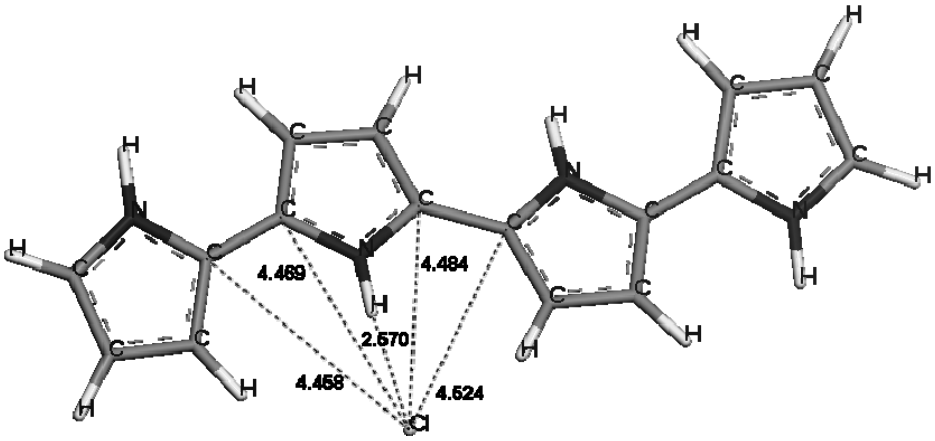

PPY-Cl

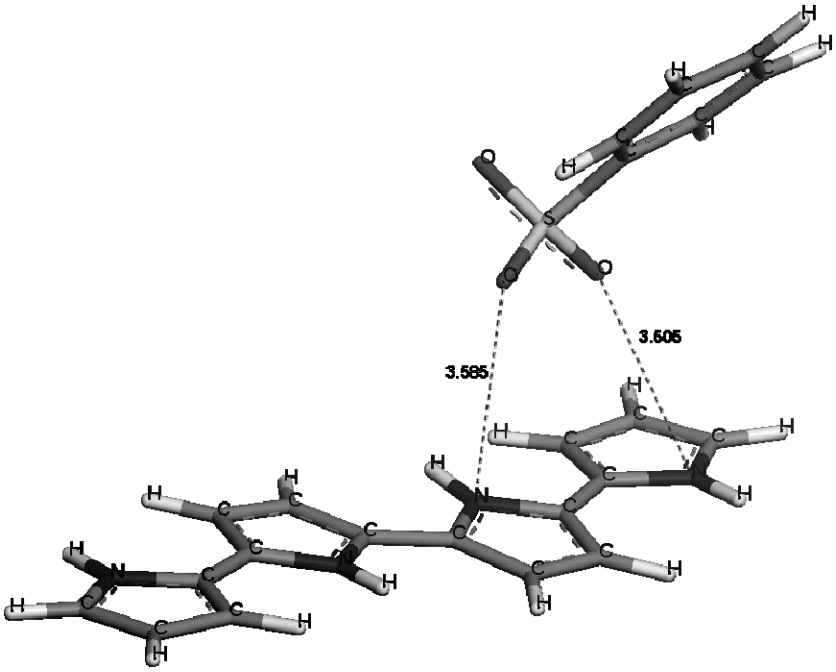

PPY-BSA I

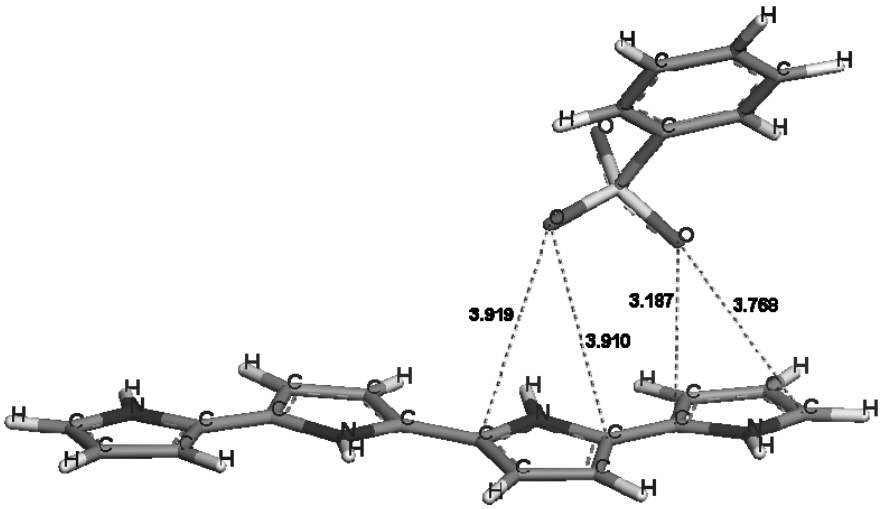

PPY-BSA II